Author Manuscript
Author Manuscript
Author Manuscript
Author Manuscript

HHS Public Access
Author manuscript
Methods Cell Biol. Author manuscript; available in PMC 2020 May 17.

Published in final edited form as:
Methods Cell Biol. 2019 ; 153: 205–229. doi:10.1016/bs.mcb.2019.04.008.

Analysis of primary cilia in renal tissue and cells

Luciane M. Silva[†], **Wei Wang**[†], **Bailey A. Allard**, **Tana S. Pottorf**, **Damon T. Jacobs**, **Pamela V. Tran**[*]

Department of Anatomy and Cell Biology, The Jared Grantham Kidney Institute, University of Kansas Medical Center, Kansas City, KS, United States

Abstract

Primary cilia are singular, sensory organelles that extend from the plasma membrane of most quiescent mammalian cells. These slender, microtubule-based organelles receive and transduce extracellular cues and regulate signaling pathways. Primary cilia are critical to the development and function of many tissue types, and mutation of ciliary genes causes multi-system disorders, termed ciliopathies. Notably, renal cystic disease is one of the most common clinical features of ciliopathies, highlighting a central role for primary cilia in the kidney. Additionally, acute kidney injury and chronic kidney disease are associated with altered primary cilia lengths on renal epithelial cells, suggesting ciliary dynamics and renal physiology are linked. Here we describe methods to examine primary cilia in kidney tissue and in cultured renal cells. We include immunofluorescence and scanning electron microscopy to determine ciliary localization of proteins and cilia structure. Further, we detail cellular assays to measure cilia assembly and disassembly, which regulate cilia length.

1 Introduction

Primary cilia appear as antenna-like appendages extending from the surface of nearly all cell types. While once thought to be vestigial structures, these small, micron-long organelles have been recognized to be vital for human development and health (Badano, Mitsuma, Beales, & Katsanis, 2006). Primary cilia transduce light, and mechanical and chemical cues (Poole, Flint, & Beaumont, 1985), tune signaling pathways (Goetz & Anderson, 2010), and are important regulators of cell cycle (Pan, Seeger-Nukpezah, & Golemis, 2013), cell differentiation, and cell-cell communication (Viau et al., 2018).

The diminutive size of primary cilia has made microscopy instrumental to illuminating its complex architecture and protein composition. Three major compartments—the basal body, the transition zone, and the axoneme—comprise the cilium (Fig. 1). When cells enter G0/G1, the mother centriole matures and differentiates into the basal body of the primary cilium, attaching to the apical plasma membrane through transition fibers (Deane, Cole, Seeley, Diener, & Rosenbaum, 2001). The basal body serves as the microtubule nucleation site of the ciliary axoneme. Adjacent to the basal body is the transition zone, characterized by the presence of Y-shaped links that connect the microtubules of the axoneme to the

[*]Corresponding author: ptran@kumc.edu.
[†]These authors contributed equally.

Author Manuscript Author Manuscript Author Manuscript Author Manuscript

ciliary membrane. The transition zone regulates the ciliary entry of proteins, and together with the transition fibers, forms the "ciliary gate," which establishes and maintains the unique protein composition of the cilium (Hsiao, Tuz, & Ferland, 2012; Reiter, Blacque, & Leroux, 2012; Szymanska & Johnson, 2012; Williams et al., 2011). Finally, the axoneme is comprised of nine microtubule doublets and is ensheathed by a ciliary membrane that contains a composition of phospholipids and signaling proteins distinct from that of the plasma membrane (Guemez-Gamboa, Coufal, & Gleeson, 2014).

Extension and maintenance of the ciliary axoneme requires intraflagellar transport (IFT), which is the bi-directional transport of protein cargo (structural and signaling components) along the microtubules (Goetz & Anderson, 2010; Malicki & Johnson, 2017; Pedersen & Rosenbaum, 2008). Anterograde IFT transports cargo from the base to the ciliary tip and is powered by the kinesin motor, while retrograde IFT returns proteins to the ciliary base and is powered by cytoplasmic dynein (Pazour, Wilkerson, & Witman, 1998). IFT complex B (IFT172, IFT88, IFT81, IFT80, IFT74, IFT57, IFT54, IFT52, IFT46, IFT27, and IFT20) associates with the kinesin motor in anterograde IFT (Cole et al., 1998). IFT complex A (IFT144, IFT140, IFT139, IFT122, IFTA-1, and IFT43) mediates retrograde IFT (Blacque et al., 2006; Tran et al., 2008) and also ciliary entry of signaling and membrane-associated proteins (Fu, Wang, Kim, Li, & Dynlacht, 2016; Mukhopadhyay et al., 2010). Another ciliary protein complex is the BBsome (BBS1, BBS2, BBS4, BBS5, BBS7, BBS8, BBS10, and BBIP10), which traffics signaling molecules to the cilium and throughout the ciliary membrane (Jin et al., 2010; Su et al., 2014; Xu et al., 2015).

Mutation and dysfunction of any of these ciliary components cause ciliopathies, which are syndromic diseases that can manifest cerebral and cognitive defects, retinal degeneration, craniofacial abnormalities, skeletal dysplasia, obesity, hypogonadism, and cysts of the pancreas, liver, and kidney (Waters & Beales, 2011). The inclusion and severity of a clinical feature appear to vary with the affected ciliary compartment, gene and mutation, which may reflect the cell-specific roles of ciliary proteins. Yet renal cysts are among the most common clinical features.

Scanning electron microscopy of renal tissue has demonstrated that primary cilia protrude from the apical membranes of most tubular epithelial cells and range in length from 2 to 7μm, depending on the tubular segment (Pazour et al., 2000). Fluorescence and scanning electron microscopy have also been instrumental in revealing the aberrant ciliary structure and protein composition in diseased states. In renal cystic diseases caused by mutation of genes that are critical to cilia assembly, such as in nephronophthisis, cilia are typically shortened or absent (Davis et al., 2011; Srivastava, Molinari, Raman, & Sayer, 2017). In contrast, in Polycystic Kidney Disease (PKD), which is caused by mutation of genes which encode proteins that localize to primary cilia, but are not required for cilia assembly, certain signaling molecules are often reduced or absent from otherwise structurally intact primary cilia (Cai et al., 2014; Freedman et al., 2013).

Cilia length misregulation has also emerged as a component of renal disease. Two PKD mouse models, *jck* and *Pkd1*$^{RC/RC}$, which harbors a human Autosomal Dominant PKD mutation, have lengthened renal primary cilia (Hopp et al., 2012; Smith et al., 2006).

Author Manuscript Author Manuscript Author Manuscript Author Manuscript

Intriguingly, pharmacological shortening and genetic ablation of cilia in *jck* mutants and in *Pkd1* and *Pkd2* conditional knock-out mice, respectively, attenuated the PKD phenotype (Husson et al., 2016; Ma, Tian, Igarashi, Pazour, & Somlo, 2013). Cilia length of renal tubular cells is also changed in acute kidney injury and chronic kidney disease, and is modulated dynamically during renal injury and repair (Han et al., 2017; Park, 2018; Verghese et al., 2009; Verghese, Weidenfeld, Bertram, Ricardo, & Deane, 2008). Interestingly, *Pkd1* and *Pkd2* heterozygous mice are sensitized to acute ischemia-reperfusion kidney injury (Bastos et al., 2009; Prasad, McDaid, Tam, Haylor, & Ong, 2009). Multiple factors, including intracellular Ca^{2+} and cAMP, oxidative stress, hormones and cytokines, have been demonstrated to alter ciliary length of renal epithelial cells (Besschetnova et al., 2010; Kim et al., 2013; Upadhyay et al., 2014). Thus, although the connection between cilia length and renal disease is incompletely understood, cilia length appears to reflect a dynamic process that must be finely regulated to sustain renal tubular integrity and function.

In light of the importance of primary cilia to kidney biology, we present methods that have been used to successfully visualize and analyze primary cilia structure, protein composition and assembly in renal tissue and cells. In particular, we detail protocols for immunofluorescence, preparation of tissue for scanning electron microscopy, shRNA-mediated gene knock-down, and cilia assembly/disassembly assays.

2 Visualization of primary cilia in renal tissue

2.1 Immunofluorescence on kidney sections

2.1.1 Overview—In 1898, renal primary cilia protruding into the tubular lumen were first observed by Zimmerman in iron hematoxylin-stained kidney sections (Zimmermann, 1898). In 1941, the first fluorescent antibody was developed by Coons, Creech, and Jones (1941), which paved the way for immunofluorescence, now the most commonly used method for visualizing primary cilia. Immunofluorescence enables the visualization of ciliary compartments and examination of ciliary localization of proteins. Such experiments are often done on tissue of novel cilia mutants or to determine the effect of certain treatments or conditions. An advantage of performing immunofluorescence on kidney sections is that tubular segments can be distinguished using tubule-specific fluorescent labels or antibodies in combination with ciliary antibodies (Fig. 2). This is useful to determine whether primary cilia of a particular tubular segment are affected under a certain condition, and since cilia lengths differ with tubular segment, to ensure that primary cilia of the same tubular segment are being compared between wild-type and mutant kidneys.

Renal tissue immunofluorescence can be performed on sections of either unfixed frozen tissue or fixed tissue (Nasr, Fidler, & Said, 2018). Often the deciding factor is the ability of the primary antibody to recognize its antigen, which can be more difficult in fixed tissue. On the other hand, fixation allows for better morphology. Following fixation and sectioning of paraffin-embedded tissue, antigen retrieval is performed to disrupt cross-links caused by fixation, unmasking epitopes. Tissue is then incubated in blocking buffer to minimize non-specific binding of antibodies that will be used to label molecules within the tissue. Two types of labeling can be used: (1) a primary antibody that is conjugated to a fluorophore or (2) a primary antibody and a secondary antibody that is conjugated to a fluorophore and

Author Manuscript Author Manuscript Author Manuscript Author Manuscript

recognizes the species in which the primary antibody was made. Using secondary antibodies provides higher sensitivity since several secondary antibodies can bind to a single primary antibody, amplifying the signal.

Renal tubular and ciliary markers commonly used in tissue sections are provided in Table 1. Renal tubular markers include both primary antibodies and lectins. Ciliary markers include acetylated α-tubulin, which labels the stable microtubules of the ciliary axoneme (Pazour et al., 2002; Qian et al., 2005; Schraml et al., 2009; Verghese et al., 2009), ARL13B, a small ciliary GTPase of Arf/Arl family that localizes to the ciliary membrane (Caspary et al., 2007), and IFT88, a component of the IFT-B complex that localizes punctately throughout the axoneme (Taulman et al., 2001).

Following immunofluorescence, sections can be viewed using conventional epifluorescent, confocal, or super-resolution microscopy. Advantages of confocal microscopy compared to epi-fluorescent microscopy are focused illumination in the specimen, reduced background and greater resolution (White, Amos, & Fordham, 1987). These qualities have made confocal immunofluorescence the more commonly used technique in published tissue immunofluorescence images. Super-resolution microscopes are more costly than confocal microscopes, but provide nanometer scale resolution and have proven extremely useful in detailing the architecture of the transition zone of primary cilia (Yang et al., 2015).

Below we describe the materials, reagents and protocols that work in our experience with mouse kidneys.

2.1.2 Materials and reagents

- Paraformaldehyde (PFA) (MP Biomedicals) or 10% formalin (Fisher)
- Phosphate Buffered Saline (PBS) (Fisher BioReagents)
- Ethanol (Decon Laboratories)
- Xylene (FisherScientific)
- Surgipath Paraplast (Leica)
- Tissue embedding cassettes (Fisher)
- Tri-sodium citrate (Fisher BioReagents)
- Hydrochloric acid (HCl) (Acros Organics)
- Tween20 (Fisher BioReagents)
- 4′,6-diamidino-2-phenylindole (DAPI)-Fluoromount-G (Electron Microscopy Sciences)
- Bovine albumin (BSA) (Sigma)
- Superfrost Plus microscope slides (Fisherbrand)
- Tissue processor (Leica)
- Paraffin embedding station (Leica)

Author Manuscript Author Manuscript Author Manuscript Author Manuscript

- Microtome (Leica)
- Food steamer (Oster)
- Slide holder and staining dish (Tissue-Tek)
- PAP pen (GeneTex)
- No. 1.5 cover glasses, rectangles (Fisherbrand)

2.1.3 Tissue fixation, processing and sectioning

1. Dissect kidneys and remove renal capsules.
2. Bisect kidneys longitudinally and place in freshly made 4% paraformaldehyde or in 10% formalin for 3–7 days.
3. Rinse kidneys 2× in 70% ethanol. Kidneys can remain in 70% ethanol for an indefinite amount of time, until processed.
4. Place tissues in embedding cassette and immerse cassettes in 70% ethanol in a beaker, until cassettes are transferred to tissue processor.
5. Place cassettes with tissue in tissue processor. Tissue will be dehydrated through an ethanol series, cleared in xylene and infiltrated with paraffin (70% ethanol—30min, 80% ethanol—30min, 95% ethanol—30min (3×), 100% ethanol—30min (3×), xylene—30min—(2×), Surgipath Paraplast—30min (3×) at 57°C)
6. Embed tissue in paraffin.
7. Section tissue using a microtome (5–8μm thicknesses according to preference).
8. Let freshly cut sections float in 40°C distilled water bath, which will remove any wrinkles from tissue section. Place glass slide beneath section and gently bring up out of water. Place slides on a slide warmer at 40°C.
9. Incubate slides in 40°C air incubator for 1–3 days. This will enable tissue to adhere to glass slide. Store slides in slide box until ready to use.

2.1.4 Antigen retrieval—Following tissue deparaffinization and rehydration, antigen retrieval is performed to allow antigen in formalin-fixed tissues to become available to immunolabeling.

1. De-paraffinize tissue sections (xylene—3min (2×)) and rehydrate through an ethanol series to distilled water (100% ethanol—3min—(2×), 90% ethanol—3min, 70% ethanol—3min, 50% ethanol—3min, distilled H_2O—2min).
2. Add autoclaved distilled water to food steamer and turn on the steamer. This will warm up the steamer prior to putting in the slides.
3. Add 200mL antigen retrieval solution (tri-sodium citrate solution, pH 6.0) to a tissue staining dish (plastic rectangular dish). To make 1L of antigen retrieval solution, add 2.94g of tri-sodium citrate to 850mL autoclaved distilled H_2O.

Author Manuscript Author Manuscript Author Manuscript Author Manuscript

Adjust pH with HCl to obtain pH 6.0. Add distilled H_2O to obtain 1L of solution. Add 500μL of Tween20.

4. Microwave antigen retrieval buffer in staining dish without slides for 1min at maximum power or until solution begins to boil.
5. Place small piece of autoclave tape on staining dish, then insert slide holder with slides into staining dish. Place staining dish with slides in steamer and steam for 25min.
6. Remove staining dish from steamer. Stripes on autoclave tape should be black, indicating steamer reached appropriate temperature. Let solution cool on bench.
7. Gently rinse slides with autoclaved distilled H_2O by moving slides to a staining dish containing autoclaved distilled H_2O. Repeat nine times.
8. Place tissue slides in PBS. If immunofluorescence will not be done immediately, slides can be stored in PBS in staining dish at 4°C for up to a few days.

2.1.5 Immunofluorescence—The immunofluorescence procedure must be carried out in a humid chamber. For example, the humid chamber can consist of a slide box with paper towels dampened with water placed at the bottom of the slide box. Place slides with tissue sections on top of the grooves of the slide box. Ensure that the slide box closes tightly, so that there is no space between the cover/top and the bottom of the closed slide box. If space is observed, then parafilm or saran wrap the sides of the closed box during ≥1h incubations, so that tissue sections do not dry out.

1. Encircle tissue with a liquid-repellent slide marker pen or PAP pen.
2. Wash 3× with PBS (5min each).
3. Block with 1–2% BSA in PBS for 1h at room temperature or overnight at 4°C.
4. Incubate with primary antibody (diluted in 1–2% BSA in PBS) overnight at 4°C.
5. Wash 3× with PBS (5min each).
6. Incubate with secondary antibody (diluted in 1–2% BSA in PBS) for 1h.
7. Wash 3× with PBS (5min each).
8. Mount tissue with DAPI-Fluoromount G. If several tissue sections are on a single slide, use a single rectangular coverslip to mount/cover all tissue sections.

2.2 Scanning electron microscopy

2.2.1 Overview—In 1935, Scanning Electron Microscopy (SEM) was first described by Knoll (Knoll, 1935). Over the decades, instruments and sample preparation techniques have improved significantly. SEM provides nanometer-scale resolution of the surface of cells and tissues (Hollenberg & Erickson, 1973), making SEM a gold standard for determining presence or absence of primary cilia, as well as cilia shape and length (Caspary et al., 2007; Hopp et al., 2012; Huangfu et al., 2003; Tran et al., 2014) (Fig. 3).

Author Manuscript Author Manuscript Author Manuscript Author Manuscript

To preserve the surface of the sample and allow imaging under electron exposure, common steps to specimen preparation are fixation, dehydration, mounting and coating. Exact conditions for each of these steps can be varied to optimize imaging depending on the sample type (Hollenberg & Erickson, 1973). Fixatives preserve the surface structure. Dehydration methods, such as air drying and critical point drying, remove fluid from the sample, since fluid is incompatible with the vacuum inside the microscope and will disturb the image. Air drying is typically done by submersing the sample in volatile liquid, such as an ethanol series. The critical point drying method utilizes a specific transitional fluid, such as CO_2 or Freon, and high pressure to dehydrate the specimen. Samples are then mounted onto metal stubs, e.g. aluminum, which allows samples to be inserted into the microscope. Once mounted, samples are coated with carbon or gold to allow for even charging of the surface during exposure to electrons in the scanning electron microscope.

Below we describe the materials, reagents and protocol used to prepare mouse tissue for imaging by a scanning electron microscope, and the use of NIH Image J software to quantify cilia length.

2.2.2 Materials and reagents

- Ketamine (provided by Laboratory Animal Resources of institution)
- Xylazine (provided by Laboratory Animal Resources of institution)
- Two 22G needles (Becton Dickinson & CO)
- Two 10mL syringes (Becton Dickinson & CO)
- Phosphate Buffered Saline (PBS) (Fisher BioReagents)
- Glutaraldehyde (Electron Microscopy Sciences)
- Cacodylate (Electron Microscopy Sciences)
- Osmium tetroxide (Electron Microscopy Sciences)
- Ethanol (Decon Laboratories)
- Critical point dryer (Electron Microscopy Sciences)
- NIH Image J software

2.2.3 Mouse tissue perfusion and fixation

1. Dilute ketamine (stock concentration of 100mg/mL) 1:5 in PBS and xylazine (stock concentration of 20mg/mL) 1:1 in PBS. Prepare a 1:1 ketamine: xylazine cocktail. Inject 100μL drug cocktail/10g mouse body weight into peritoneum. Wait a few minutes for drugs to take effect. Squeeze foot of mouse with forceps and observe if mouse responds. Begin procedure only once animal no longer responds to stimulus.
2. Open the animal's abdominal cavity and thorax to expose the heart.
3. Pierce the animal's right atrium with a 22G needle (Fig. 4) and observe that blood flows out.

Author Manuscript Author Manuscript Author Manuscript Author Manuscript

4. Attach 22G needle to a 10mL syringe filled with 10mL PBS and insert needle into animal's left ventricle. Gently press down on syringe to gradually allow all of 10mL PBS to circulate throughout body of mouse. Watch for liver to change color and pale. This will indicate that blood is being cleared from circulation.
5. Switch syringe to one that contains 7mL of cold fixative (2% glutaraldehyde in 0.1M cacodylate buffer, pH range 6.8–7.4, stored at 4°C). Gently press down on syringe to gradually allow fixative to circulate body and replace PBS. Wait around 5min.
6. Collect small pieces of the tissues of interest and store in fixative (2% glutaraldehyde in 0.1M cacodylate buffer, pH range 6.8–7.4) in a glass vial at 4°C until ready to proceed.
7. In fume hood, wash tissue with 0.1M cacodylate buffer for 10min (2×).
8. In fume hood, replace cacodylate buffer with 1% osmium tetroxide fixative for 30min.
9. Rinse tissue 2× with distilled water.

2.2.4 Specimen processing and mounting

1. Dehydrate sample using an ethanol series: 50%, 70%, 95%, 100% (2×)—10–20min each step, depending on tissue size. Larger tissue samples require 20min.
2. Dehydrate samples in a critical point dryer.
3. Mount the samples onto metal stubs and sputter coat with gold to prevent tissue from being charged by the electrical field of the microscope.
4. View and image samples using a scanning electron microscope.

2.2.5 Quantifying cilia length

1. Run NIH ImageJ software.
2. In the menu, select "File."
3. Open SEM image with scale bar as a TIF file.
4. From menu, select "Straight line tool" and mark a cilium. (Since cilia are not always straight, >1 straight-line measurements may be necessary for some cilia. In these cases, add each straight-line measurement for a given cilium).
5. From menu, select "Analyze" and "Measure."
6. Convert ImageJ units to μm, using measurements of scale bar.

3 Visualization and analysis of primary cilia in cultured renal cells

3.1 Immunofluorescence on cultured cells

3.1.1 Overview—Several renal epithelial cell lines derived from human, dog, mouse and pig have proven useful for studying primary cilia (Gaush, Hard, & Smith, 1966; Graham,

Author Manuscript Author Manuscript Author Manuscript Author Manuscript

Smiley, Russell, & Nairn, 1977; Nielsen et al., 1998; Rauchman, Nigam, Delpire, & Gullans, 1993; Reif et al., 2011; Stoos, Naray-Fejes-Toth, Carretero, Ito, & Fejes-Toth, 1991) (Table 2). In immunofluorescence experiments, an advantage of using cultured renal cells over fixed renal tissue is that more antibodies have proven successful in detecting their antigens, allowing for more components of primary cilia to be analyzed. In addition to antibodies against acetylated α-tubulin, ARL13B and IFT88, discussed in Section 2.1.1, centriole markers, γ-tubulin, which binds the minus ends of microtubules, and pericentrin, which localizes to the pericentriolar material, have proven successful on cultured cells (Breslow, Koslover, Seydel, Spakowitz, & Nachury, 2013; Ishikawa, Thompson, Yates, & Marshall, 2012). Antibodies against additional IFT proteins, including IFT52, IFT81, IFT140, and against BBSome components, BBS2 and BBS5, have also yielded positive results (Silva et al., 2018). These antibodies and their sources are provided in Table 3. Often signaling molecules transit through primarycilia and increase their presence in primary cilia in response to a ligand or stimulus. While the ciliary presence of signaling molecules may not always be possible to capture in tissue sections, cultured cells allow the ciliary presence of signaling molecules to be examined following addition of a ligand to the culture media (Silva et al., 2018). Cells can also be stimulated with fluid flow, cytokines, Ca^{2+} and cAMP, and other modulators to examine effect on primary cilia length and protein composition (Besschetnova et al., 2010; Upadhyay et al., 2014; Wann & Knight, 2012). Another advantage of using cultured cells is that cilia assembly and disassembly, which are tightly coordinated with the cell cycle, can also be examined. Cilia assembly begins in G1/G0 and disassembly begins at the G1-S transition, and these phases of the cell cycle can be induced by omitting serum from the culture media, and adding serum back to the culture media after serum starvation, respectively. The balance between cilia assembly and disassembly regulates cilia length (Mirvis, Stearns, & James Nelson, 2018; Spalluto, Wilson, & Hearn, 2013).

Below we describe the materials, reagents and protocols for examining cilia assembly/disassembly and performing immunofluorescence in cultured cells.

3.1.2 Materials and reagents

- 12mm No. 1.5 cover glasses, circle (Fisherbrand)
- 50mL conical tube (Fisher)
- 10M or 1M HCl (Fisher)
- Poly-L-lysine (Sigma-Aldrich)
- Ethanol (Decon Laboratories)
- 10cm cell culture dish (Fisher)
- 24-well cell culture dish (Fisher)
- Phosphate-buffered saline (PBS) (Fisher)
- Paraformaldehyde (MP Biomedicals)
- Triton X-100 (Fisher BioReagents)

Author Manuscript Author Manuscript Author Manuscript Author Manuscript

- 4′,6-diamidino-2-phenylindole (DAPI)-Fluoromount-G (Electron Microscopy Sciences)
- Bovine albumin (BSA) (Sigma-Aldrich)
- Superfrost Plus microscope slides (Fisherbrand)
- 26G needle (Fisher)
- #5 forceps (Fine Science Tools)

3.1.3 Poly-l-lysine coating of coverslips—To perform immunofluorescence on cultured cells, cells are plated onto coverslips that have been acid-washed and treated with polyamino acids, such as poly-L-lysine, which promotes adherence of cells to the glass- or plastic-ware for optimal growth.

1. Preheat water bath to 50–60°C.
2. Place coverslips in a 50mL conical tube, containing 1M HCl. (Add 5mL of 10M HCL to 45mL autoclaved distilled H_2O to make 50mL 1M HCl).
3. Keep tube with coverslips in 1M HCl in 50–60°C water bath for 4–16h, inverting tube several times intermittently and gently so that individual coverslips are cleaned.
4. Cool to room temperature.
5. Replace HCl with distilled H_2O. Rinse coverslips with distilled H_2O by inverting tube several times gently, then wash for 20min (3×) with autoclaved distilled H_2O on a rocker.
6. Wash for 20min with 50% ethanol on a rocker.
7. Wash for 20min with 70% ethanol on a rocker. If needed, the protocol can be paused at this step. Keep coverslips in 70% ethanol at room temperature overnight.
8. Wash for 20min with 95% ethanol on a rocker.
9. Place coverslips in a single layer in a 10cm Petri dish.
10. Coat coverslips with 10–15mL of 1mg/mL of poly-L-lysine. Rock for at least 30min at room temperature or overnight at 4°C.
11. Wash for 10min (at least 10×) with autoclaved distilled H_2O on a rocker and then place coverslips into a 50mL conical tube.
12. Wash for 20min with 50% ethanol on a rocker.
13. Wash for 20min with 70% ethanol on a rocker.
14. Fill tube with 70% ethanol and store at room temperature.

3.1.4 Ciliogenesis—Since primary cilia begin assembly in G1/G0, serum starvation is often used to halt cell cycling and induce primary cilia synthesis.

Author Manuscript Author Manuscript Author Manuscript Author Manuscript

1. Plate cells on poly-L-lysine-coated coverslips in a 24-well plate with complete medium containing 10% FBS.
2. Two days after cells have reached 100% confluence, change medium to serum-free medium for 24h to induce ciliogenesis.
3. Fix and immunostain cells as detailed in Section 3.1.6.

3.1.5 Cilia disassembly—Disassembly of cilia begins at the G1-S transition, which can be induced in cultured cells by adding serum to the culture media following serum starvation.

1. Plate cells on 12-mm poly-lysine coated glass coverslips in a 24-well plate with complete medium containing 10% FBS.
2. Two days after cells have reached 100% confluence, change media to serum-free media for 24h to bring cells to G0 and induce ciliogenesis.
3. Following 24-h serum starvation, feed cells with media containing 10% FBS for 2h to induce cilia disassembly.
4. Fix and immunostain cells as detailed in Section 3.1.6.

3.1.6 Fixation and immunostaining—Throughout the protocol, gently add solutions to cells by touching pipette tip to side of well and remove solutions using a dropper pipette. This will help prevent cells from detaching from the coverslips.

1. Make 4% paraformaldehyde (PFA) containing 0.2% triton X-100 in PBS.
2. Rinse cells with PBS and fix cells with 4% PFA containing 0.2% triton X-100 for 10min at room temperature.
3. Rinse cells 2× with PBS.
4. Block cells with 1% BSA in PBS for 1 h at room temperature or overnight at 4 °C.
5. Incubate cells in primary antibody (diluted in 1% BSA in PBS) for 1h at room temperature or overnight at 4°C.
6. Wash cells 3× with PBS (5min each).
7. Incubate cells in secondary antibody (diluted in 1% BSA in PBS) for 1h at room temperature. For steps 7–11, minimize light exposure to reduce exciting fluorophore attached to secondary antibody.
8. Wash cells 3× with PBS (5min each).
9. Mount coverslips. Place drop of mounting medium containing 4,6-diamidino-2-phenylindole (DAPI) on a glass slide. Use bent 26G needle (bend tip of needle) to gently lift up one slide of coverslip from well and fine forceps to remove coverslip from well, and place coverslip upside down on top of mounting medium on slide. Up to six coverslips (12mm) can be mounted onto one slide.

Author Manuscript Author Manuscript Author Manuscript Author Manuscript

10. Seal edges of coverslips with nail polish. (This step is optional.)

11. Store slides in dark at 4°C before viewing.

3.1.7 Epi-fluorescent, confocal or super-resolution microscopy—Epi-fluorescent microscopy can be used to analyze cilia formation and protein localization. Cilia microscopy images can be taken using a 60× oil immersion. Confocal laser scanning microscopy uses lasers for illumination to increase resolution. Confocal microscopy can also obtain an image from just one focal plane to generate images with less background. For better resolution of images, a confocal laser microscope with a 60× oil immersion objective is recommended (Fig. 5). Alternatively, super-resolution microscopy provides even greater resolution (Fig. 6).

3.1.8 Quantification of ciliated cells—Following cilia assembly/disassembly and immunofluorescence protocols, the percentage of ciliated cells can be determined by dividing the number of cells that have primary cilia (i.e., acetylated α-tubulin positive) by the number of total cells (i.e., DAPI positive) within a field, and multiplying by 100.

3.2 Modifying cilia using shRNA

3.2.1 Overview—Knocking down gene expression using shRNA in cells is useful to elucidate the cellular function of a novel gene (Tran et al., 2008). Additionally, knock-down cell lines can be used to determine the mechanisms by which a gene regulates cilia structure, assembly/disassembly, and protein composition in various contexts, such as in the presence or absence of a stimulus.

Efficient shRNA-mediated knock-down results in approximately 70% knock-down of gene expression. A key step is to identify an effective shRNA sequence for the gene of interest. This usually requires assessing several shRNA sequences for one gene. The RNAi Consortium (TRC) at the Broad Institute has created the TRC shRNA library, in which shRNA sequences against human and mouse genes have been cloned into the pLKO.1 lentiviral expression plasmid. These shRNA-containing pLKO.1 plasmids (targeting 15,000 human genes and 13,000 mouse genes) are commercially available from Sigma-Aldrich. Alternatively, the Broad Institute has designed a “GPP (Genetic Perturbation Platform) web portal—Design hairpins” bioinformatics site (https://portals.broadinstitute.org/gpp/public/seq/search) that uses an algorithm to identify shRNA sequences for any given transcript. If the latter method is chosen, the shRNA sequence needs to be cloned into the *Age*I/*Eco*RI sites of the pLKO.1 lentiviral vector. To make lentiviruses, the pLKO.1 vector, either empty or containing a scrambled sequence as control, or containing the shRNA (transfer vector), is transfected together with two other plasmids, VSV-G (envelope vector), and dR8. 2 (packaging vector), into 293T cells (Stewart et al., 2003). Supernatant containing the lentiviruses are collected 48h after transfection and are then used to infect target cells. Lentiviruses are advantageous by having the capability to infect both dividing and non-dividing cells, and in generating stable integration of the shRNA into the genome.

Below we describe the protocols for lentivirus production, shRNA-mediated gene knock-down in cultured cells, and clonal selection of cells. Since lentivirus production requires

Author Manuscript Author Manuscript Author Manuscript Author Manuscript

BSL2+ designation of working areas, we also provide BSL2+ protocols for working with lentiviruses and disposing of contaminated materials.

3.2.2 Materials and reagents

- pLKO.1 puro plasmid (Addgene)
- pLKO.1 puro plasmid containing shRNA (Sigma-Aldrich)
- pCMV-dR8.2 dvpr (Addgene)
- pCMV-VSV-G plasmid (Addgene)
- 293T cells (ATCC)
- Target cells (e.g., IMCD)
- 10cm cell culture plates (Fisher)
- Fugene (Promega)
- 10mL syringe (Fisher)
- 0.45μm filter (Fisher)
- Polybrene (Sigma-Aldrich)
- Puromycin (Fisher)
- 25cm cell culture plates (Fisher)
- Cloning disks (VWR)
- Trypsin (Fisher)
- 24-well plate (Fisher)
- 6-well plate (Fisher)
- Bleach
- Ethanol (Decon Laboratories)
- Sterile #5 forceps (Fine Science Tools)

3.2.3 Making lentiviruses expressing shRNA and infecting target cells

1. In an Eppendorf tube, add 3-plasmids (4.2μg pLKO.1, 7.4μg dR8.2, 0.4μg VSVG), then autoclaved distilled H_2O to 40μL total volume, then mix.
2. In another Eppendorf tube, add 24μL Fugene, 160μL serum-free media, then mix.
3. Add DNA to Fugene and serum-free media, mix (total volume is 224μL). Let sit 25–45min. at room temperature.
4. Add 224μL to a 10cm plate of 293T cells at 70% confluency. (Plate 1:5 dilution of a confluent 10cm plate the day before.)
5. Incubate 48h (no media change).

Author Manuscript Author Manuscript Author Manuscript Author Manuscript

6. Attach 10mL syringe to 0.45μm filter.
7. Harvest virus by collecting supernatant with syringe and filter supernatant through 0.45μm filter. This will typically yield 9mL of virus. Virus can be used immediately or flash-frozen in 3mL aliquots and stored at −80°C.
8. Infect target cells. For a 10cm plate of approximately 60–75% confluent target cells (usually plated 1:5 dilution from a confluent 10cm plate the day before), use 3mL virus. Add 1.5μL polybrene to 3mL virus before placing on cells. Incubate 3–4h.
9. After incubation, add 7mL media or change media completely.
10. Next day, change media completely.
11. Once cells reach confluency, passage cells (1:5) into 10cm plates containing media with puromycin (10mg/mL) to select for infected cells.
12. The following day, feed cells with media containing puromycin.
13. Culture cells 4–10 days after infection to see effect of RNAi.

3.2.4 Clonal selection of knock-down cells—Since the multiplicity of infection (MOI) will differ between cells, i.e., different numbers of lentiviruses will infect individual cells, we recommend clonal selection of cells to obtain cell lines with homogeneous knock-down.

1. Plate cells at very low confluency in a 25cm cell culture plate, so that cells are isolated.
2. Monitor plates daily and feed cells every 3 days. Isolated cells should eventually form islands of cells (i.e., clones). When approximately 50–100 cells comprise an island or clone, individual clones can be “picked.”
3. Immerse cloning disks in trypsin. Aspirate media from cell culture plate. Using sterile forceps, place cloning disk over an individual clone for 5min. Pick up cloning disk with sterile forceps and place in a 24-well plate with media. Let cells expand over a few days. When cells are confluent, trypsinize cells and plate cells in a 6-well dish. When cells are confluent, trypsinize cells and plate cells in a 10 cm cell culture dish.
4. Verify gene knock-down in cells by performing qPCR or Western blot for target gene or protein.

3.2.5 BSL2+ working procedures and disposal of contaminated reagents— The BSL2+ designated laboratory space and project should be approved by the institution. From lentiviral production until target cells have been passaged twice, BSL2+ working procedures should be implemented.

1. Wear appropriate PPE (Personal protective equipment), consisting of disposable plastic lab coat and two pairs of gloves. Plastic lab coat can be used for up to 1

Author Manuscript Author Manuscript Author Manuscript Author Manuscript

week, then discarded in biohazard bin. Discard gloves in biohazard bin. Wash hands outside BSL2+ working space.

2. Prepare fresh 10% bleach daily. Soak all lentivirus-contaminated materials (plasticware—plates, serological pipettes, syringes, filters) in 10% bleach for 30min before disposing solids in biohazard bag. Decontaminate all liquids with 10% bleach for 30min before discarding in sink.

3. Solids in biohazard bag must be autoclaved twice.

4. Wipe down flow hood with 10% bleach, followed by 70% ethanol.

4 Conclusion

Fluorescence and electron microscopy on fixed tissue and cells will continue to be essential and feasible techniques to examine primary cilia phenotypes. The generation of additional antibodies that successfully recognize their antigens and more widespread availability of super-resolution microscopes will augment the effectiveness of fluorescence microscopy. Tagging endogenous loci with fluorophores using methodologies, like CRISPR, combined with in vivo imaging at the super-resolution level will likely provide the next powerful methodologies to discover additional details of the architecture of ciliary subdomains, ciliary protein composition and ciliary dynamics.

Acknowledgment

This work is supported by R01 DK103033 (to P.V.T.).

References

Badano JL, Mitsuma N, Beales PL, & Katsanis N (2006). The ciliopathies: An emerging class of human genetic disorders. Annual Review of Genomics and Human Genetics, 7, 125–148. 10.1146/annurev.genom.7.080505.115610.

Bastos AP, Piontek K, Silva AM, Martini D, Menezes LF, Fonseca JM, et al. (2009). Pkd1 haploinsufficiency increases renal damage and induces microcyst formation following ischemia/reperfusion. Journal of the American Society of Nephrology, 20(11), 2389–2402. 10.1681/ASN.2008040435. [PubMed: 19833899]

Besschetnova TY, Kolpakova-Hart E, Guan Y, Zhou J, Olsen BR, & Shah JV (2010). Identification of signaling pathways regulating primary cilium length and flow-mediated adaptation. Current Biology, 20(2), 182–187. 10.1016/j.cub.2009.11.072. [PubMed: 20096584]

Blacque OE, Li C, Inglis PN, Esmail MA, Ou G, Mah AK, et al. (2006). The WD repeat-containing protein IFTA-1 is required for retrograde intraflagellar transport. Molecular Biology of the Cell, 17(12), 5053–5062. 10.1091/mbc.E06-06-0571. [PubMed: 17021254]

Breslow DK, Koslover EF, Seydel F, Spakowitz AJ, & Nachury MV (2013). An in vitro assay for entry into cilia reveals unique properties of the soluble diffusion barrier. The Journal of Cell Biology, 203(1), 129 10.1083/jcb.201212024. [PubMed: 24100294]

Cai Y, Fedeles SV, Dong K, Anyatonwu G, Onoe T, Mitobe M, et al. (2014). Altered trafficking and stability of polycystins underlie polycystic kidney disease. Journal of Clinical Investigation, 124(12), 5129–5144. 10.1172/JCI67273. [PubMed: 25365220]

Caspary T, Larkins CE, & Anderson KV (2007). The graded response to Sonic Hedgehog depends on cilia architecture. Developmental Cell, 12(5), 767–778. 10.1016/j.devcel.2007.03.004. [PubMed: 17488627]

Author Manuscript Author Manuscript Author Manuscript Author Manuscript

Cole DG, Diener DR, Himelblau AL, Beech PL, Fuster JC, & Rosenbaum JL (1998). Chlamydomonas kinesin-II-dependent intraflagellar transport (IFT): IFT particles contain proteins required for ciliary assembly in Caenorhabditis elegans sensory neurons. Journal of Cell Biology, 141(4), 993–1008. [PubMed: 9585417]

Coons AH, Creech HJ, & Jones RN (1941). Immunological properties of an antibody containing a fluorescent group. Proceedings of the Society for Experimental Biology and Medicine, 47(2), 200–202.

Davis EE, Zhang Q, Liu Q, Diplas BH, Davey LM, Hartley J, et al. (2011). TTC21B contributes both causal and modifying alleles across the ciliopathy spectrum. Nature Genetics, 43(3), 189–196. 10.1038/ng.756. [PubMed: 21258341]

Deane JA, Cole DG, Seeley ES, Diener DR, & Rosenbaum JL (2001). Localization of intraflagellar transport protein IFT52 identifies basal body transitional fibers as the docking site for IFT particles. Current Biology, 11(20), 1586–1590. [PubMed: 11676918]

Freedman BS, Lam AQ, Sundsbak JL, Iatrino R, Su X, Koon SJ, et al. (2013). Reduced ciliary polycystin-2 in induced pluripotent stem cells from polycystic kidney disease patients with *PKD1* mutations. Journal of the American Society of Nephrology, 24(10), 1571–1586. 10.1681/ASN.2012111089. [PubMed: 24009235]

Fu W, Wang L, Kim S, Li J, & Dynlacht BD (2016). Role for the IFT-A complex in selective transport to the primary cilium. Cell Reports, 17(6), 1505–1517. 10.1016/j.celrep.2016.10.018. [PubMed: 27806291]

Gaush CR, Hard WL, & Smith TF (1966). Characterization of an established line of canine kidney cells (MDCK). Proceedings of the Society for Experimental Biology and Medicine, 122(3), 931–935. [PubMed: 5918973]

Goetz SC, & Anderson KV (2010). The primary cilium: A signalling centre during vertebrate development. Nature Reviews. Genetics, 11(5), 331–344. 10.1038/nrg2774.

Graham FL, Smiley J, Russell WC, & Nairn R (1977). Characteristics of a human cell line transformed by DNA from human adenovirus type 5. The Journal of General Virology, 36(1), 59–74. 10.1099/0022-1317-36-1-59. [PubMed: 886304]

Guemez-Gamboa A, Coufal NG, & Gleeson JG (2014). Primary cilia in the developing and mature brain. Neuron, 82(3), 511–521. 10.1016/j.neuron.2014.04.024. [PubMed: 24811376]

Han SJ, Jang HS, Seu SY, Cho HJ, Hwang YJ, Kim JI, et al. (2017). Hepatic ischemia/reperfusion injury disrupts the homeostasis of kidney primary cilia via oxidative stress. Biochimica et Biophysica Acta - Molecular Basis of Disease, 1863(7), 1817–1828. 10.1016/j.bbadis.2017.05.004. [PubMed: 28495528]

Hollenberg MJ, & Erickson AM (1973). The scanning electron microscope: Potential usefulness to biologists. A review. The Journal of Histochemistry and Cytochemistry, 21(2), 109–130. 10.1177/21.2.109. [PubMed: 4571700]

Hopp K, Ward CJ, Hommerding CJ, Nasr SH, Tuan HF, Gainullin VG, et al. (2012). Functional polycystin-1 dosage governs autosomal dominant polycystic kidney disease severity. Journal of Clinical Investigation, 122(11), 4257–4273. 10.1172/JCI64313. [PubMed: 23064367]

Hsiao YC, Tuz K, & Ferland RJ (2012). Trafficking in and to the primary cilium. Cilia, 1(1), 4 10.1186/2046-2530-1-4. [PubMed: 23351793]

Huangfu D, Liu A, Rakeman AS, Murcia NS, Niswander L, & Anderson KV (2003). Hedgehog signalling in the mouse requires intraflagellar transport proteins. Nature, 426(6962), 83–87. 10.1038/nature02061. [PubMed: 14603322]

Husson H, Moreno S, Smith LA, Smith MM, Russo RJ, Pitstick R, et al. (2016). Reduction of ciliary length through pharmacologic or genetic inhibition of CDK5 attenuates polycystic kidney disease in a model of nephronophthisis. Human Molecular Genetics, 25(11), 2245–2255. 10.1093/hmg/ddw093. [PubMed: 27053712]

Ishikawa H, Thompson J, Yates JR, & Marshall WF (2012). Proteomic analysis of mammalian primary cilia. Current Biology, 22(5), 414–419. 10.1016/j.cub.2012.01.031. [PubMed: 22326026]

Jin H, White SR, Shida T, Schulz S, Aguiar M, Gygi SP, et al. (2010). The conserved Bardet-Biedl syndrome proteins assemble a coat that traffics membrane proteins to cilia. Cell, 141(7), 1208–1219. 10.1016/j.cell.2010.05.015. [PubMed: 20603001]

Author Manuscript Author Manuscript Author Manuscript Author Manuscript

Kim JI, Kim J, Jang HS, Noh MR, Lipschutz JH, & Park KM (2013). Reduction of oxidative stress during recovery accelerates normalization of primary cilia length that is altered after ischemic injury in murine kidneys. American Journal of Physiology. Renal Physiology, 304(10), F1283–F1294. 10.1152/ajprenal.00427.2012. [PubMed: 23515720]

Knoll M (1935). Charge potential and secondary emissions of electron irradiated bodies. Physikalische Zeitschrift, 36, 861–869.

Ma M, Tian X, Igarashi P, Pazour GJ, & Somlo S (2013). Loss of cilia suppresses cyst growth in genetic models of autosomal dominant polycystic kidney disease. Nature Genetics, 45(9), 1004–1012. 10.1038/ng.2715. [PubMed: 23892607]

Malicki JJ, & Johnson CA (2017). The cilium: Cellular antenna and central processing unit. Trends in Cell Biology, 27(2), 126–140. 10.1016/j.tcb.2016.08.002. [PubMed: 27634431]

Mirvis M, Stearns T, & James Nelson W (2018). Cilium structure, assembly, and disassembly regulated by the cytoskeleton. The Biochemical Journal, 475(14), 2329–2353. 10.1042/BCJ20170453. [PubMed: 30064990]

Mukhopadhyay S, Wen X, Chih B, Nelson CD, Lane WS, Scales SJ, et al. (2010). TULP3 bridges the IFT-A complex and membrane phosphoinositides to promote trafficking of G protein-coupled receptors into primary cilia. Genes and Development, 24(19), 2180–2193. 10.1101/gad.1966210. [PubMed: 20889716]

Nasr SH, Fidler ME, & Said SM (2018). Paraffin immunofluorescence: A valuable ancillary technique in renal pathology. Kidney International Reports, 3(6), 1260–1266. 10.1016/j.ekir.2018.07.008. [PubMed: 30450452]

Nielsen R, Birn H, Moestrup SK, Nielsen M, Verroust P, & Christensen EI (1998). Characterization of a kidney proximal tubule cell line, LLC-PK1, expressing endocytotic active megalin. Journal of the American Society of Nephrology, 9(10), 1767–1776. [PubMed: 9773777]

Pan J, Seeger-Nukpezah T, & Golemis EA (2013). The role of the cilium in normal and abnormal cell cycles: Emphasis on renal cystic pathologies. Cellular and Molecular Life Sciences, 70(11), 1849–1874. 10.1007/s00018-012-1052-z. [PubMed: 22782110]

Park KM (2018). Can tissue cilia lengths and urine cilia proteins be markers of kidney diseases? Chonnam Medical Journal, 54(2), 83–89. 10.4068/cmj.2018.54.2.83. [PubMed: 29854673]

Pazour GJ, Dickert BL, Vucica Y, Seeley ES, Rosenbaum JL, Witman GB, et al. (2000). Chlamydomonas IFT88 and its mouse homologue, polycystic kidney disease gene tg737, are required for assembly of cilia and flagella. Journal of Cell Biology, 151(3), 709–718. [PubMed: 11062270]

Pazour GJ, San Agustin JT, Follit JA, Rosenbaum JL, & Witman GB (2002). Polycystin-2 localizes to kidney cilia and the ciliary level is elevated in Tg737(orpk) mice with polycystic kidney disease. Molecular Biology of the Cell, 13, 326a–327a.

Pazour GJ, Wilkerson CG, & Witman GB (1998). A dynein light chain is essential for the retrograde particle movement of intraflagellar transport (IFT). Journal of Cell Biology, 141(4), 979–992. [PubMed: 9585416]

Pedersen LB, & Rosenbaum JL (2008). Intraflagellar transport (IFT) role in ciliary assembly, resorption and signalling. Current Topics in Developmental Biology, 85, 23–61. 10.1016/S0070-2153(08)00802-8. [PubMed: 19147001]

Plotnikova OV, Seo S, Cottle DL, Conduit S, Hakim S, Dyson JM, et al. (2015). INPP5E interacts with AURKA, linking phosphoinositide signaling to primary cilium stability. Journal of Cell Science, 128(2), 364–372. 10.1242/jcs.161323. [PubMed: 25395580]

Poole CA, Flint MH, & Beaumont BW (1985). Analysis of the morphology and function of primary cilia in connective tissues: A cellular cybernetic probe? Cell Motility, 5(3), 175–193. [PubMed: 4005941]

Prasad S, McDaid JP, Tam FW, Haylor JL, & Ong AC (2009). *Pkd2* dosage influences cellular repair responses following ischemia-reperfusion injury. The American Journal of Pathology, 175(4), 1493–1503. 10.2353/ajpath.2009.090227. [PubMed: 19729489]

Qian CN, Knol J, Igarashi P, Lin F, Zylstra U, Teh BT, et al. (2005). Cystic renal neoplasia following conditional inactivation of apc in mouse renal tubular epithelium. Journal of Biological Chemistry, 280(5), 3938–3945. 10.1074/jbc.M410697200. [PubMed: 15550389]

Author Manuscript Author Manuscript Author Manuscript Author Manuscript

Rauchman MI, Nigam SK, Delpire E, & Gullans SR (1993). An osmotically tolerant inner medullary collecting duct cell line from an SV40 transgenic mouse. The American Journal of Physiology, 265(3 Pt 2), F416–F424. 10.1152/ajprenal.1993.265.3.F416. [PubMed: 8214101]

Reif GA, Yamaguchi T, Nivens E, Fujiki H, Pinto CS, & Wallace DP (2011). Tolvaptan inhibits ERK-dependent cell proliferation, Cl(–) secretion, and in vitro cyst growth of human ADPKD cells stimulated by vasopressin. American Journal of Physiology. Renal Physiology, 301(5), F1005–F1013. 10.1152/ajprenal.00243.2011. [PubMed: 21816754]

Reiter JF, Blacque OE, & Leroux MR (2012). The base of the cilium: Roles for transition fibres and the transition zone in ciliary formation, maintenance and compartmentalization. EMBO Reports, 13(7), 608–618. 10.1038/embor.2012.73. [PubMed: 22653444]

Schraml P, Frew IJ, Thoma CR, Boysen G, Struckmann K, Krek W, et al. (2009). Sporadic clear cell renal cell carcinoma but not the papillary type is characterized by severely reduced frequency of primary cilia. Modern Pathology, 22(1), 31–36. 10.1038/modpathol.2008.132. [PubMed: 18660794]

Seixas C, Choi SY, Polgar N, Umberger NL, East MP, Zuo X, et al. (2015). Arl13b and the exocyst interact synergistically in ciliogenesis. Molecular Biology of the Cell, 27(2), 308–320. 10.1091/mbc.e15-02-0061. [PubMed: 26582389]

Silva LM, Jacobs DT, Allard BA, Fields TA, Sharma M, Wallace DP, et al. (2018). Inhibition of hedgehog signaling suppresses proliferation and microcyst formation of human autosomal dominant polycystic kidney disease cells. Scientific Reports, 8(1), 4985 10.1038/s41598-018-23341-2. [PubMed: 29563577]

Smith LA, Bukanov NO, Husson H, Russo RJ, Barry TC, Taylor AL, et al. (2006). Development of polycystic kidney disease in juvenile cystic kidney mice: Insights into pathogenesis, ciliary abnormalities, and common features with human disease. Journal of the American Society of Nephrology, 17(10), 2821–2831. 10.1681/ASN.2006020136. [PubMed: 16928806]

Sohara E, Luo Y, Zhang J, Manning DK, Beier DR, & Zhou J (2008). Nek8 regulates the expression and localization of polycystin-1 and polycystin-2. Journal of the American Society of Nephrology, 19(3), 469–476. 10.1681/ASN.2006090985. [PubMed: 18235101]

Spalluto C, Wilson DI, & Hearn T (2013). Evidence for reciliation of RPE1 cells in late G1 phase, and ciliary localisation of cyclin B1. FEBS Open Bio, 3, 334–340. 10.1016/j.fob.2013.08.002.

Srivastava S, Molinari E, Raman S, & Sayer JA (2017). Many genes-one disease? Genetics of nephronophthisis (NPHP) and NPHP-associated disorders. Frontiers in Pediatrics, 5, 287 10.3389/fped.2017.00287. [PubMed: 29379777]

Stewart SA, Dykxhoorn DM, Palliser D, Mizuno H, Yu EY, An DS, et al. (2003). Lentivirus-delivered stable gene silencing by RNAi in primary cells. RNA (New York, N.Y.), 9(4), 493–501. 10.1261/rna.2192803.

Stoos BA, Naray-Fejes-Toth A, Carretero OA, Ito S, & Fejes-Toth G (1991). Characterization of a mouse cortical collecting duct cell line. Kidney International, 39(6), 1168–1175. [PubMed: 1654478]

Su X, Driscoll K, Yao G, Raed A, Wu M, Beales PL, et al. (2014). Bardet-Biedl syndrome proteins 1 and 3 regulate the ciliary trafficking of polycystic kidney disease 1 protein. Human Molecular Genetics, 23(20), 5441–5451. 10.1093/hmg/ddu267. [PubMed: 24939912]

Szymanska K, & Johnson CA (2012). The transition zone: An essential functional compartment of cilia. Cilia, 1(1), 10 10.1186/2046-2530-1-10. [PubMed: 23352055]

Taulman PD, Haycraft CJ, Balkovetz DF, & Yoder BK (2001). Polaris, a protein involved in left-right axis patterning, localizes to basal bodies and cilia. Molecular Biology of the Cell, 12(3), 589–599. 10.1091/mbc.12.3.589. [PubMed: 11251073]

Tran PV, Haycraft CJ, Besschetnova TY, Turbe-Doan A, Stottmann RW, Herron BJ, et al. (2008). THM1 negatively modulates mouse sonic hedgehog signal transduction and affects retrograde intraflagellar transport in cilia. Nature Genetics, 40(4), 403–410. 10.1038/ng.105. [PubMed: 18327258]

Tran PV, Talbott GC, Turbe-Doan A, Jacobs DT, Schonfeld MP, Silva LM, et al. (2014). Downregulating hedgehog signaling reduces renal cystogenic potential of mouse models. Journal

Author Manuscript Author Manuscript Author Manuscript Author Manuscript

of the American Society of Nephrology, 25(10), 2201–2212. 10.1681/ASN.2013070735. [PubMed: 24700869]

Upadhyay VS, Muntean BS, Kathem SH, Hwang JJ, Aboualaiwi WA, & Nauli SM (2014). Roles of dopamine receptor on chemosensory and mechanosensory primary cilia in renal epithelial cells. Frontiers in Physiology, 5, 72 10.3389/fphys.2014.00072. [PubMed: 24616705]

Verghese E, Ricardo SD, Weidenfeld R, Zhuang J, Hill PA, Langham RG, et al. (2009). Renal primary cilia lengthen after acute tubular necrosis. Journal of the American Society of Nephrology, 20(10), 2147–2153. 10.1681/ASN.2008101105. [PubMed: 19608704]

Verghese E, Weidenfeld R, Bertram JF, Ricardo SD, & Deane JA (2008). Renal cilia display length alterations following tubular injury and are present early in epithelial repair. Nephrology, Dialysis, Transplantation, 23(3), 834–841. 10.1093/ndt/gfm743.

Viau A, Bienaime F, Lukas K, Todkar AP, Knoll M, Yakulov TA, et al. (2018). Cilia-localized LKB1 regulates chemokine signaling, macrophage recruitment, and tissue homeostasis in the kidney. EMBO Journal, 37(15), e98615 10.15252/embj.201798615. [PubMed: 29925518]

Wann AKT, & Knight MM (2012). Primary cilia elongation in response to interleukin-1 mediates the inflammatory response. Cellular and Molecular Life Sciences: CMLS, 69(17), 2967–2977. 10.1007/s00018-012-0980-y. [PubMed: 22481441]

Waters AM, & Beales PL (2011). Ciliopathies: An expanding disease spectrum. Pediatric Nephrology, 26(7), 1039–1056. 10.1007/s00467-010-1731-7. [PubMed: 21210154]

White JG, Amos WB, & Fordham M (1987). An evaluation of confocal versus conventional imaging of biological structures by fluorescence light microscopy. The Journal of Cell Biology, 105(1), 41–48. [PubMed: 3112165]

Williams CL, Li C, Kida K, Inglis PN, Mohan S, Semenec L, et al. (2011). MKS and NPHP modules cooperate to establish basal body/transition zone membrane associations and ciliary gate function during ciliogenesis. Journal of Cell Biology, 192(6), 1023–1041. 10.1083/jcb.201012116. [PubMed: 21422230]

Xu Q, Zhang Y, Wei Q, Huang Y, Li Y, Ling K, et al. (2015). BBS4 and BBS5 show functional redundancy in the BBSome to regulate the degradative sorting of ciliary sensory receptors. Scientific Reports, 5, 11855 10.1038/srep11855. [PubMed: 26150102]

Yang TT, Su J, Wang WJ, Craige B, Witman GB, Tsou MF, et al. (2015). Super-resolution pattern recognition reveals the architectural map of the ciliary transition zone. Scientific Reports, 5, 14096 10.1038/srep14096. [PubMed: 26365165]

Yu F, Sharma S, Skowronek A, & Erdmann KS (2016). The serologically defined colon cancer antigen-3 (SDCCAG3) is involved in the regulation of ciliogenesis. Scientific Reports, 6, 35399 10.1038/srep35399. [PubMed: 27767179]

Zimmermann KW (1898). Beitrage zur Kenntniss einiger Drusen und Epithelien. Archiv für Mikroskopische Anatomie, 52, 552–706.

Author Manuscript Author Manuscript Author Manuscript Author Manuscript

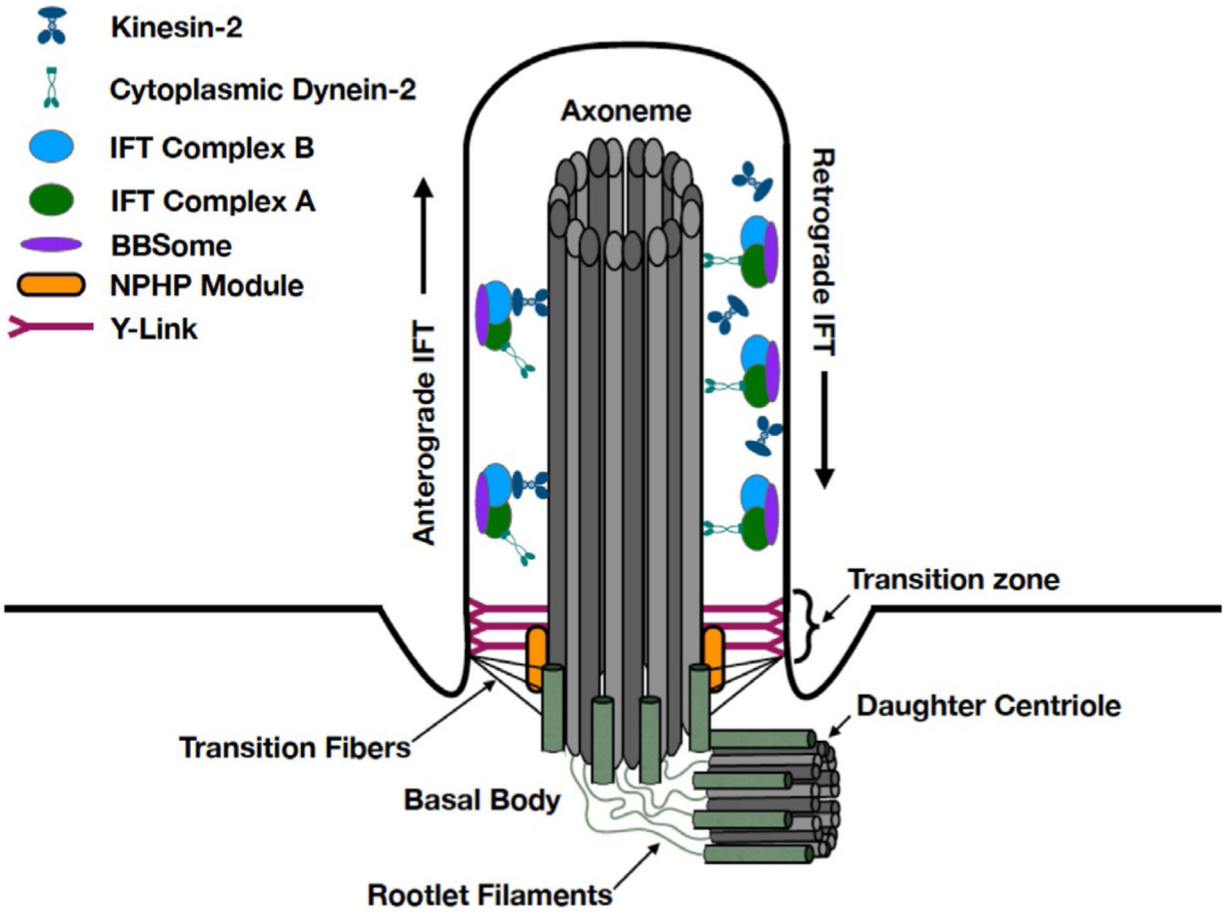

FIG. 1.
Diagram of primary cilia structure.

Author Manuscript Author Manuscript Author Manuscript Author Manuscript

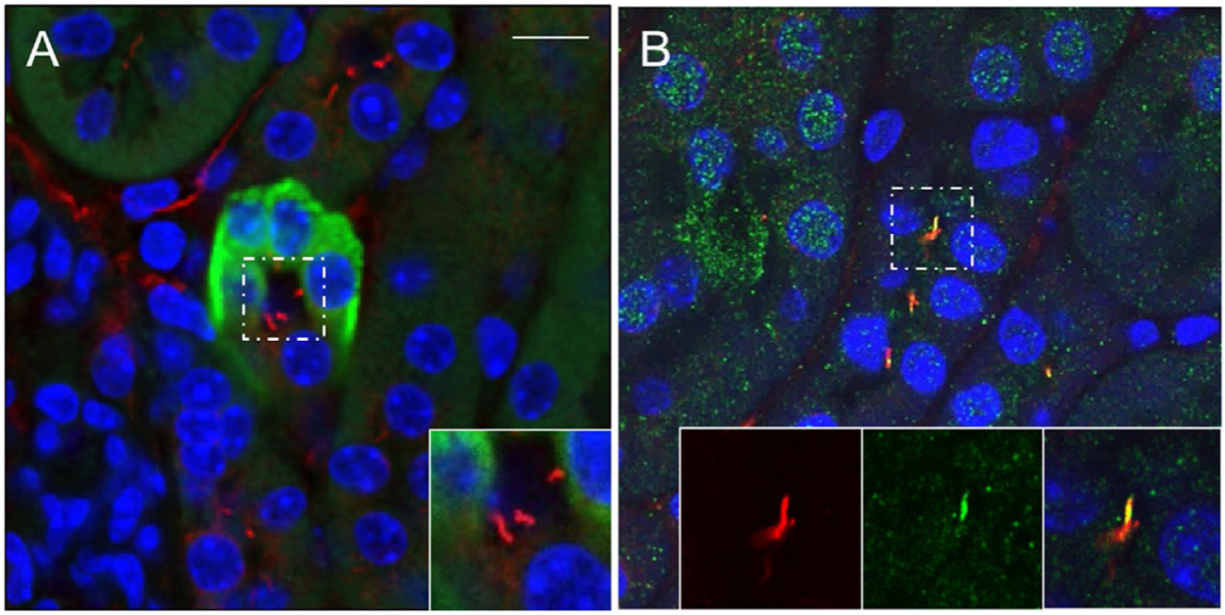

FIG. 2.

Confocal images of primary cilia in mouse kidney sections. (A) Staining for Ac-α-tubulin (red), a marker of the ciliary axoneme, and for *Dolichos biflorus* agglutinin (DBA; green), a marker for collecting duct. (B) Immunostaining for Ac-α-tubulin (red) and IFT81 (green). Nuclei are stained with 4′,6-diamidino-2-phenylindole (DAPI; blue). Inset shows magnified view of boxed regions. Scale bar=10μm. Images obtained using a Nikon A1 confocal laser microscope.

Author Manuscript Author Manuscript Author Manuscript Author Manuscript

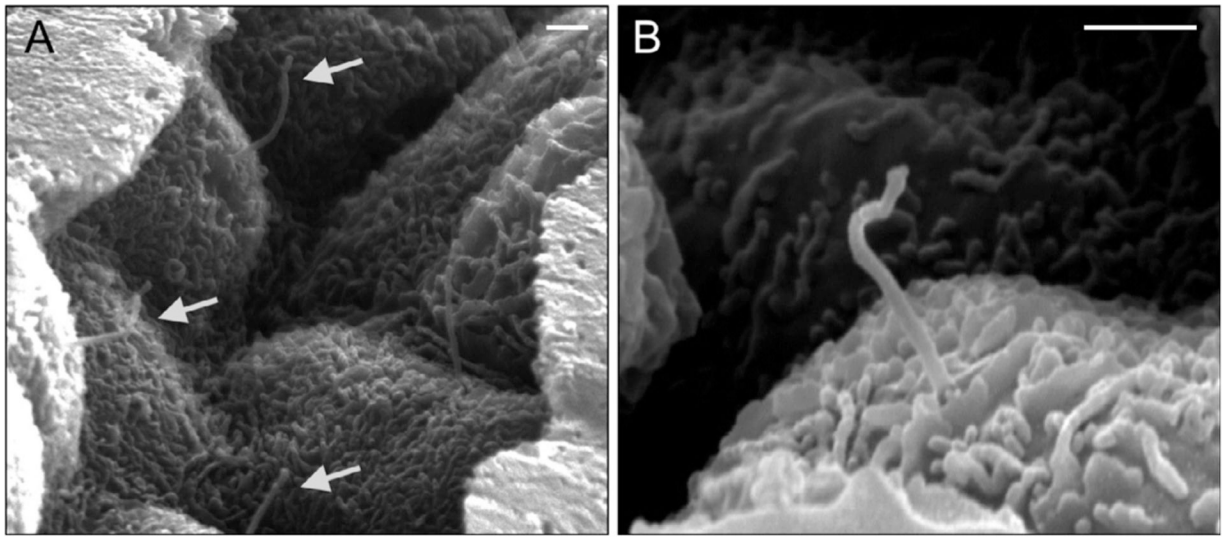

FIG. 3.

Scanning electron micrographs of primary cilia in mouse renal tubules. (A) Arrows point to a primary cilium. (B) Higher magnification of a primary cilium. Scale bars = 1μm. Images were obtained using a Hitachi S-2700 Scanning Electron Microscope attached to a Quartz PCI digital camera.

Author Manuscript Author Manuscript Author Manuscript Author Manuscript

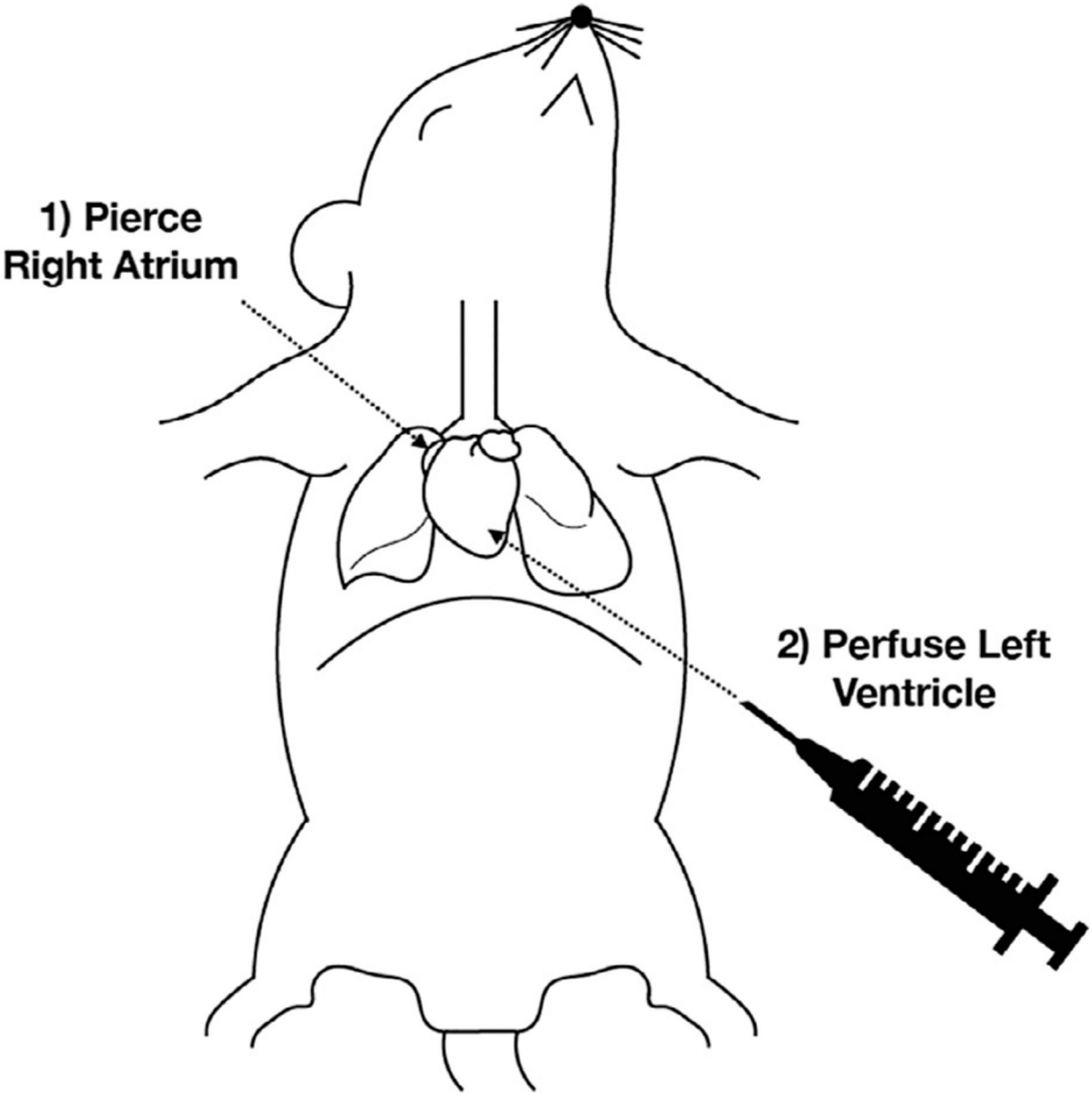

FIG. 4.
Schematic of mouse perfusion.

Author Manuscript Author Manuscript Author Manuscript Author Manuscript

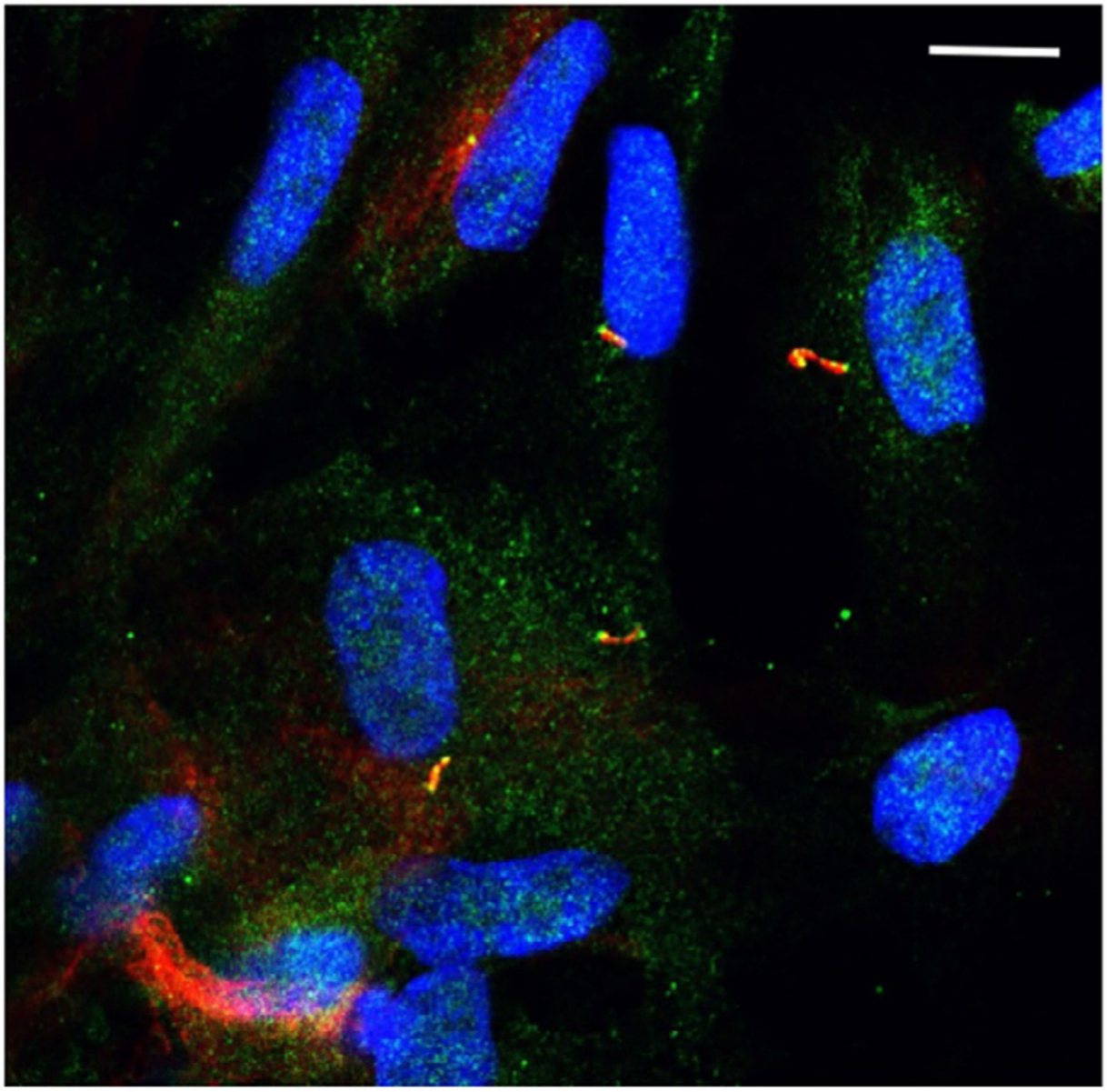

FIG. 5.

Confocal image of primary cilia of cultured primary Normal Human Kidney (NHK) cells. Immunostaining for Ac-α-tubulin (red) and IFT81 (green) to mark primary cilia. Nuclei are stained with DAPI (blue). Scale bar = 10 μm. Cells were imaged using a Leica TCS SPE confocal microscope configured on a DM550 Q upright microscope.

Author Manuscript Author Manuscript Author Manuscript Author Manuscript

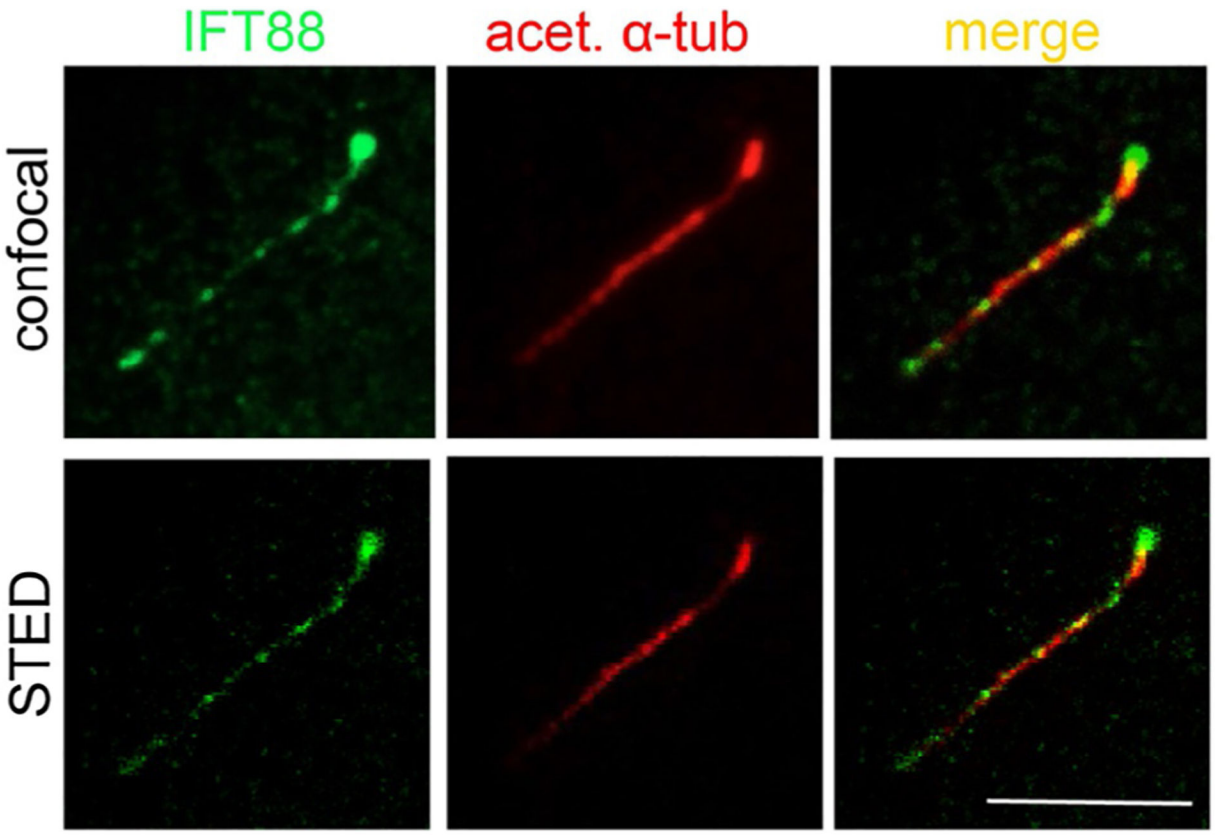

FIG. 6.

Comparison of confocal and STED images of a primary cilium on a primary Autosomal Dominant Polycystic Kidney Disease (ADPKD) cell. Scale bar = 5μm. Resolution is much improved by STED microscopy. Images were obtained using a Leica TCS SP8 STED 3×.

Author Manuscript Author Manuscript Author Manuscript Author Manuscript

Table 1

Markers of primary cilia and renal tubules.

Antibody or lectin	Company	Localization	References
Acetylated α-tubulin	Sigma-Aldrich	Axoneme	Pazour, San Agustin, Follit, Rosenbaum, and Witman (2002), Qian et al. (2005), Schraml et al. (2009), and Verghese et al. (2009)
ARL13b	Proteintech	Ciliary membrane	Caspary, Larkins, and Anderson (2007) and Ma et al. (2013)
IFT88	Proteintech	Punctate along axoneme	Taulman, Haycraft, Balkovetz, and Yoder (2001)
Aquaporin-2	Santa-Cruz Biotechnology	Collecting duct	Verghese et al. (2009)
Tamm-Horsfall Protein (THP)	Santa-Cruz Biotechnology	Loop of Henle	Tran et al. (2014)
Lotus tetragonolobus lectin (LTL)	Vector Laboratories	Proximal tubule	Sohara et al. (2008) and Verghese et al. (2009)
Dolichos biflorus agglutinin (DBA)	Vector Laboratories	Collecting duct	Ma et al. (2013), Sohara et al. (2008), and Verghese et al. (2009)

Author Manuscript

Author Manuscript

Author Manuscript

Author Manuscript

Table 2

Immortalized and primary renal epithelial cells.

Cell line	Description	Source	References
M-1	Murine cortical collecting duct epithelial cells	ATCC	Stoos et al. (1991)
IMCD-3	Murine inner medullary collecting duct epithelial cells	ATCC	Rauchman et al. (1993)
LLC-PK1	Porcine proximal tubule epithelial cells	ATCC	Nielsen et al. (1998)
MDCK	Madin-Darby canine kidney epithelial cells	ATCC	Gaush et al. (1966)
NHK/ADPKD	Primary cortical epithelial cells from normal human kidney (NHK) or Autosomal Dominant PKD (ADPKD)	KUMC	Graham et al. (1977) and Reif et al. (2011)

Author Manuscript Author Manuscript Author Manuscript Author Manuscript

Table 3

Markers of primary cilia.

Antibody	Company	Cilia structure	References
Acetylated-α-tubulin	Sigma-Aldrich	Axoneme	Ishikawa et al. (2012), Seixas et al. (2015), Silva et al. (2018), and Yu, Sharma, Skowronek, and Erdmann (2016)
γ-tubulin	Sigma-Aldrich	Centrioles	Breslow et al. (2013)
Pericentrin	Covance	Centrioles	Ishikawa et al. (2012)
ARL13B	Proteintech	Ciliary membrane	Seixas et al. (2015)
INPP5E	Proteintech	Ciliary membrane	Plotnikova et al. (2015)
IFT52	Proteintech	Axoneme	Silva et al. (2018)
IFT81	Proteintech	Axoneme	Silva et al. (2018)
IFT88	Proteintech	Axoneme	Silva et al. (2018)
IFT140	Proteintech	Axoneme	Silva et al. (2018)
BBS2	Proteintech	Axoneme	Silva et al. (2018)
BBS5	Proteintech	Axoneme	Silva et al. (2018)